

RESEARCH

Open Access



# Hippocampal gray matter volume alterations in patients with first-episode and recurrent major depressive disorder and their associations with gene profiles

Fenfen Sun<sup>1,2†</sup>, Yifan Shuai<sup>3†</sup>, Jingru Wang<sup>2</sup>, Jin Yan<sup>2</sup>, Bin Lin<sup>4</sup>, Xinyun Li<sup>5</sup> and Zhiyong Zhao<sup>6\*</sup>

## Abstract

**Background** Recent studies indicate that patients with first-episode drug-naïve (FEDN) and recurrent major depressive disorder (R-MDD) exhibit distinct atrophy patterns in the hippocampal subregions along the proximal-distal axis. However, it remains unclear whether such differences occur along the long axis and how they may relate to specific genes.

**Methods** In the present study, we analyzed T1-weighted images from 421 patients (FEDN:  $n = 232$ ; R-MDD:  $n = 189$ ) and 544 normal controls (NC) as part of the REST-meta-MDD consortium. Additionally, transcriptome maps and structural Magnetic Resonance Imaging (MRI) data of six donated brains were obtained from the Allen Human Brain Atlas (AHBA). We first identified changes in gray matter volume (GMV) within the hippocampus of both FEDN and R-MDD patients and then integrated these findings with AHBA transcriptome data to investigate the genes associated with hippocampal GMV changes.

**Results** Compared to NC, FEDN patients displayed reduced GMV in the left hippocampal tail, whereas R-MDD patients exhibited decreased GMV in the bilateral hippocampal body and increased GMV in the bilateral hippocampal tail. Further analysis revealed that expression levels of *SYTL2* positively correlated with GMV changes in the hippocampus of FEDN patients, while *SORCS3* and *SLIT2* positively correlated with those in R-MDD.

**Conclusions** Our results suggest that GMV alterations in hippocampal subfields along the long axis differ between FEDN and R-MDD, reflecting progressive hippocampal deterioration with prolonged depression, potentially supported by the expression of specific genes. These findings offer valuable insights into the distinct neural and genetic mechanisms underlying FEDN and R-MDD, which may aid in the development of more targeted and effective treatment strategies for MDD subtypes.

**Keywords** Major depressive disorder, Hippocampal subfields, Magnetic resonance imaging, Gray matter volume, Gene expression

<sup>†</sup>Fenfen Sun and Yifan Shuai contributed equally to this work.

\*Correspondence:

Zhiyong Zhao  
zhaozhiyong\_zju@zju.edu.cn

Full list of author information is available at the end of the article



© The Author(s) 2025. **Open Access** This article is licensed under a Creative Commons Attribution-NonCommercial-NoDerivatives 4.0 International License, which permits any non-commercial use, sharing, distribution and reproduction in any medium or format, as long as you give appropriate credit to the original author(s) and the source, provide a link to the Creative Commons licence, and indicate if you modified the licensed material. You do not have permission under this licence to share adapted material derived from this article or parts of it. The images or other third party material in this article are included in the article's Creative Commons licence, unless indicated otherwise in a credit line to the material. If material is not included in the article's Creative Commons licence and your intended use is not permitted by statutory regulation or exceeds the permitted use, you will need to obtain permission directly from the copyright holder. To view a copy of this licence, visit <http://creativecommons.org/licenses/by-nc-nd/4.0/>.

## Introduction

The hippocampus (HP), a central component of the limbic system, is extensively connected to several cortical areas, including the prefrontal cortex, anterior thalamic nuclei, amygdala, basal ganglia, and hypothalamus [1]. These regions form a neuroanatomical network involved in mood regulation [2, 3]. Therefore, the hippocampus plays a significant role in various cognitive and emotional processes, and its dysfunction is commonly linked to psychiatric disorders, such as major depressive disorder (MDD) [4]. Structural imaging studies have revealed abnormalities in hippocampal volumes among MDD patients. However, some of them found unilateral volume reductions, while others reported bilateral reductions, and still others detected no significant differences in MDD patients compared to healthy controls [5, 6]. These inconsistencies may stem from variations in Magnetic Resonance Imaging (MRI) methodologies and samples, particularly the proportions of first-episode and recurrent MDD patients [5–7]. Early studies indicated that patients with multiple episodes tend to have smaller hippocampal volumes than those experiencing their first episode [8, 9], and this also was supported by a recent large-sample study showing lower hippocampal volumes in recurrent MDD patients compared to controls, while no differences were noted in first-episode patients [10]. However, another study [7] found that first-episode patients had a significantly smaller left hippocampal volume, but recurrently depressed patients showed no differences from healthy controls. These inconsistencies motivate further exploration of the relationship between depressive episodes and hippocampal volume.

Numerous studies have demonstrated that the hippocampus is a heterogeneous structure, segmented into distinct subfields along various axes. Specifically, the hippocampus can be divided into three main parts—head, body, and tail—along the long (anterior-posterior) axis [11, 12], and further into subfields including Cornu Ammonis (CA1–4), the dentate gyrus (DG), fimbria, and adjacent subiculum along the proximal-distal axis [13]. Research focused on hippocampal subfields has found that MDD patients exhibit reduced volumes in bilateral CA1–CA4, DG, and subiculum, with more pronounced changes in the left side for recurrent depression, whereas only CA2 to CA4 were reduced in first-episode depression [14]. Moreover, remitted patients showed larger pretreatment hippocampal body and tail volumes compared to those who remained non-remitted after eight weeks [15], with increased hippocampal tail volume predicting depression status and remission in major depression [4]. However, volumetric studies often treat the hippocampus as either a single anatomical entity or as multiple distinct subfields,

providing only overall or mean volume measures that may overlook critical details. A voxel-wise analysis could yield more comprehensive insights related to this disease.

Gray matter volume (GMV) serves as a widely used structural measure, reflecting the sum of cell and non-cell components, which can be accurately quantified by T1-weighted MRI. Studies combining neuroimaging and genetic data have explored associations between genetic candidates for MDD and hippocampal volume alterations. For instance, Gonul et al. reported hippocampal volume reduction in MDD patients was observed only in Val allele homozygotes of the *BDNF* Val66Met polymorphism [16]. Another study indicated that the MDD-related reduction in hippocampal volume was associated with S allele homozygotes of the *5-HTTLPR* [17]. Additionally, findings regarding hippocampal subfields revealed that *TESC* gene-regulating genetic variant (rs7294919) affects volumes of the DG and CA4 in MDD patients [18]. The high-risk rs1360780 T-allele of *FKBP5* in the hippocampus-amygdala-transition-area subfield showed a significant interaction with early life stress in MDD patients [19]. Previous studies have reported a negative correlation between the number of depressive episodes and hippocampal GMV, with more severe alterations in recurrent MDD compared to first-episode MDD [20]. However, so far, no studies have specifically examined which genes underlie the distinct alterations in intra-hippocampal GMV for first-episode and recurrent MDD.

Given that cortical gene expression patterns are highly conserved across individuals [21], several studies have linked transcriptomic data from postmortem brains with group-averaged neuroimaging maps from living subjects, revealing conserved gene expression associated with neuroimaging measures [22–24], such as GMV and functional connectivity. Importantly, a recent study has identified biological and cellular pathways consistent with known molecular neuroimaging markers through transcriptomic decoding [25], and this further confirmed the validity of the transcription-neuroimaging association approach. This allows us to investigate the relationship between gene expression profiles and alterations in intra-hippocampus GMV in MDD. Therefore, we first examined changes in intra-hippocampus GMV in first-episode and recurrent MDD patients, and subsequently integrated transcriptomic and neuroimaging data from six postmortem brains obtained from the Allen Human Brain Atlas (AHBA). Our aim was to identify genes specifically associated with alterations in hippocampal GMV in first-episode and recurrent MDD patients, respectively. We hypothesize that first-episode and recurrent MDD will show different patterns of intra-hippocampus

GMV changes along the long axis, potentially linked to distinct gene expression profiles.

## Materials and methods

### In-vivo data

The Chinese REST-meta-MDD database [26] includes 1300 MDDs and 1128 normal controls (NCs). Our exclusion criteria were as follows: (1) subjects without information on sex, age and education; (2) age below 18 or above 65; (3) low quality of fMRI data (i.e., bad spatial normalization and bad coverage); (4) excessive head motion (mean framewise displacement > 0.2 mm); (5) patients met the Diagnostic and Statistical Manual of Mental Disorders IV criteria for MDD; (6) sites with fewer than 10 subjects. We screened structural MRI data of 544 NCs and 421 MDD patients. Among the patients, 232 patients were first-episode drug-naïve (FEDN) from five sites, and 189 patients were recurrent MDD (R-MDD) from six sites. For the control group, we screened 394 NCs matched with FEDN and 427 NCs matched with R-MDD in age, sex, and site, respectively. In addition, we also screened 119 FEDN and 72 R-MDD patients, and 227 FEDN and 100 first-episode medicated (FEM) patients, with matched age, sex, education, and site. Samples of the REST meta-MDD project, consortium sites, sample size and data acquisition parameters are presented in Supplementary Table S1.

Additionally, duration of illness was available for 220 FEDN and 170 R-MDD patients; 17-item Hamilton Depression Rating Scale (HAMD) total score was available for 209 FEDN and 146 R-MDD patients; HAMD item scores were available for 111 FEDN and 102 R-MDD patients, and Hamilton Anxiety Rating Scale (HAMA) score was available for 148 FEDN and 143 R-MDD patients. All study sites obtained approval from their local institutional review boards and ethics committees, and all participants provided written informed consent at their local institutions.

### Ex-vivo data

The *ex-vivo* data comprise six donated brains, which include both transcriptomic and structural MRI data from the AHBA (<http://human.brain-map.org>). A total of 3,702 tissue samples were extracted from these brains using scalpel-based manual macro-dissection and laser microdissection. Microarray data for each tissue sample was obtained using a custom Agilent 8×60 K cDNA array chip, featuring approximately 58,692 probes to capture the expression of 20,786 genes. To minimize non-biological systematic biases while preserving biological variation, normalization was performed both within and between brains by the Allen Institute for Brain Science. Three-dimensional T1-weighted structural MRI was also

collected from the six donors shortly after death and prior to tissue dissection.

### MRI data processing

MRI images were processed using Data Processing Assistant for Resting-State fMRI (DPARSF) software following a standardized protocol [26] for all sites. Individual T1-weighted images were segmented into gray matter (GM), white matter (WM), and cerebrospinal fluid (CSF). Then, transformations from individual native space to Montreal Neurological Institute (MNI) space were computed using the Diffeomorphic Anatomical Registration Through Exponentiated Lie algebra (DARTEL) tool and applied to the GM concentration maps. Finally, the normalized GMV map was obtained by multiplying the normalized GM concentration maps by the nonlinear determinants generated during the normalization procedure. The GMV maps were resliced to a cubic voxel size of 1.5 mm and smoothed with a full width at half maximum (FWHM) Gaussian kernel of 4 mm.

### AHBA transcriptomic data preprocessing

We used the Abagen toolbox (<https://www.github.com/netneurolab/abagen>) to preprocess the transcriptomic data, which included the following steps [27, 28]: (1) updating probe-to-gene annotations; (2) applying an intensity-based filter; (3) selecting probes; (4) handling missing data; (5) normalizing samples; (6) normalizing genes; and (7) selecting stable genes. This resulted in a gene expression matrix of 188 hippocampal tissues × 10,028 genes for further analysis. The AHBA provides anatomically precise genome-wide transcription maps of the human brain, including the neocortex, basal ganglia, hippocampus, cerebellum, and brainstem. To investigate the genetic underpinnings of hippocampal GMV, we focused on 188 hippocampal tissue samples from the AHBA dataset.

### Mapping tissue samples to the human brain Atlas

The MNI coordinates for tissue samples were used to map them to the brain atlas [22, 23]. First, samples were selected by mapping each MNI coordinate provided by the AHBA to a hippocampal mask created by the Human Brainnetome Atlas [29]. Then, the Euclidean distance was calculated between each sample and every voxel within the mask, and samples with the largest distance within 1 mm were included in the study. Finally, 133 out of the 188 hippocampal samples from the AHBA were mapped to the hippocampal atlas and were included in subsequent transcription-neuroimaging analysis.

### GMV extraction for each hippocampal sample

To establish the spatial correspondence between GMV and gene expression for each tissue sample, we created a sphere centered on the MNI coordinates of the sample, with a radius of 1.5 mm (equivalent to one voxel size) on the GMV map. Since gene-GMV correlations were performed across the regions of interest (ROIs), we aimed to minimize spatial overlap between ROIs for reliable correlation analysis. As shown in Fig S1, using a radius greater than a single voxel (e.g., 2 voxels = 3 mm) led to substantial spatial overlap between ROIs. Therefore, we opted to use one single voxel as the radius. The GMV of all voxels within each sphere was averaged as the GMV for the tissue sample. If a sphere extended outside the hippocampal mask, only the voxels overlapping with the mask were included in the GMV calculation. Finally, a total of 133 spherical ROIs were defined from the six donated AHBA brains, and their GMV values were extracted.

### Identifying target genes correlated with hippocampal volume or MDD

A recent genome-wide association study (GWAS) of MDD conducted by the Psychiatric Genomics Consortium identified 44 MDD-related risk loci associated with 69 genes [30]. We first overlapped these 69 genes with the 10,028 candidate genes from the preprocessed AHBA dataset, obtaining 34 MDD-related genes. Next, we employed both prior-knowledge and data-driven methods to identify genes associated with the hippocampus: (1) Three previous GWAS studies [31–33] identified a total of 22 genes related to the hippocampal volumes. We overlapped these genes with the 10,028 candidate genes from AHBA, resulting in 13 genes; (2) We performed a Pearson correlation analysis between GMV and the expression of each gene across all 133 samples from all donors in the ex-vivo data. We found that 113 of the 10,028 genes showed significant correlations with intra-hippocampus GMV (Bonferroni correction for the number of genes). Subsequently, we validated these relationships in 794 normal in-vivo subjects. Individual GMV values for the NC group were extracted across the 133 hippocampal ROIs, and we calculated the Pearson correlation between the expression of the 113 identified genes and the GMV of each individual across all ROIs. Genes that were consistently significantly correlated (BH-FDR correction for the number of genes and subjects) in more than 90% [24] of individuals in the NC dataset were selected. To further assess whether the number of identified genes was significantly greater than the random level, we performed a spatially constrained permutation test using a null model [34], which is implemented in an open-access, Python-based software package, BrainS-MASH: Brain Surrogate Maps with Autocorrelated

Spatial Heterogeneity (<https://github.com/murraylab/brainsmash>). The process was repeated 5,000 times to generate a null distribution, and we compared the number of genes identified in the real data against this null distribution to assess statistical significance. Finally, we combined the genes associated with hippocampal volume identified in steps (1) and (2) with the 34 MDD-related genes as targeted genes for subsequent analysis.

### Statistical analysis

We conducted a voxel-wise t-test within a hippocampal mask (the number of voxels = 5336) using a linear mixed model, controlling for age, sex, education, whole-brain volume as covariates, and site as a random effect, to compare the intra-hippocampus GMV differences between FEDN and NC, between R-MDD and NC, between FEDN and FEM, and between R-MDD and FEDN, respectively. We also used the Combat harmonization method to control the batch effect inherent for between-group comparisons again. And, we performed Leave-One-Site-Out Cross Validation (LOSOCV) for each paired group comparison to evaluate the reproducibility of GMV differences between groups. Specifically, one site was excluded from the sample, and group comparisons were based on the remaining, permuted samples. This process resulted in five tests for FEDN vs. NC and six tests for R-MDD vs. NC, respectively. For each voxel, we calculated the proportion of tests in which the voxel exhibited significant group differences and expressed this as the reproducibility ratio. Then, we performed a voxel-wise partial correlation analysis between hippocampal GMV and various clinical measures, including duration of illness, HAMA, HAMD total score and its each item in each patient subgroup, controlling for age, sex, education and head motion as the covariates. BH-FDR multiple comparison correction ( $p < 0.05$ ) was applied to control the false positive rate. Subsequently, patient-control differences were computed as the ratio of change in hippocampal GMV between the patients and control populations (i.e.,  $\Delta\text{GMV} = [\text{patients} - \text{controls}] / [\text{controls}]$ , namely difference between groups in averaged GMV) [23] per hippocampal ROI across two independent sites for each paired groups (i.e., FEDN vs. NC, R-MDD vs. NC and FEDN vs. R-MDD). Finally, we assessed the associations between the expression of target genes and  $\Delta\text{GMV}$  using Pearson's correlation analysis across all 133 hippocampal ROIs. The whole pipeline of data analysis in this study is presented in Fig. 1.

## Results

### Demographic and imaging information of participants

This study included three independent datasets: (1) six postmortem brains from the AHBA with both



transcriptomic and structural MRI data and (2) 794 healthy subjects and 421 MDDs from the REST-meta-MDD consortium. Structural MRI data were available for all datasets. Demographic information for in-vivo datasets are presented in Table S2. Both FEDN and R-MDD showed no significant differences in age and sex ( $p > 0.05$ ), but lower educations ( $p < 0.05$ ) compared to NCs. Two patient subgroups were matched in age, sex, education and HAMD total score ( $p > 0.05$ ), with a longer duration of illness ( $p < 0.05$ ) in R-MDD than FEDN groups.

### MDD-related alterations in hippocampal GMV and their correlations with clinical assessments

According to the subfield segmentations (Fig. S2) reported in our previous studies [35, 36], which used a group-level independent component analysis in an fMRI dataset including a total of 63 healthy subjects (age =  $23.33 \pm 7.82$  years; male/female = 22:41; education =  $12.60 \pm 3.54$  years), we found that compared with NC group, the FEDN group exhibited decreased GMV in the hippocampal tail (Fig. 2A). In contrast, the R-MDD group showed decreased GMV in the hippocampal body and increased GMV in the hippocampal tail (Fig. 2B). These differences showed a high reproducibility in the Leave-One-Site-Out Cross Validation (LOSOCV) tests (Fig. 3). Also, they were also validated by using the Combat harmonization method to control the site effect. No significant differences in hippocampal GMV were found between FEDN and FEM groups and between FEDN and R-MDD groups (adjusted  $p > 0.05$ ). Partial correlation analysis revealed that GMV in the head and body of the hippocampus was positively correlated with item 8 (which assesses retardation in movement and speech observed during the interview of the HAMD) (Fig. 4A) in the FEDN group. In the R-MDD group, GMV in the body and tail of the hippocampus was positively correlated with the total score of the HAMA (Fig. 4B).

### The genes showing specific to GMV alteration in MDD subtypes

As mentioned in Method section, we first identified a total of 52 target genes associated with either the hippocampus or MDD. Then, we further found that the expression value of *SYTL2* positively correlated with the intra-hippocampus  $\Delta$ GMV in the FEDN, while

the expression values of *SORCS3* and *SLIT2* positively correlated with the intra-hippocampus  $\Delta$ GMV in the R-MDD. Furthermore, the expression levels of five genes—*SORCS3*, *SCG2*, *SLIT2*, *SYTL2*, and *FAM110B*—demonstrated significant correlations with the intra-hippocampus  $\Delta$ GMV of R-MDD versus FEDN (Bonferroni correction,  $p < 0.05$ ) (Fig. 5). These genes were primarily involved in neuronal signaling, synaptic transmission and cell migration (Table 1). Notably, these findings have been validated by two independent datasets.

### Discussion

The present study employed a transcriptomic-neuroimaging approach to investigate the molecular basis of alterations related to MDD subtypes in intra-hippocampus GMV. We found that: 1) compared to controls, the FEDN group exhibited decreased GMV in the hippocampal tail, while the R-MDD group showed increased GMV in the same region; conversely, the hippocampal body displayed decreased GMV in R-MDD but no significant changes in FEDN; 2) the GMV of the medial hippocampal head in FEDN positively correlated with HAMD (item 8), whereas the GMV of the hippocampal body in R-MDD positively correlated with the HAMA; and 3) alterations in intra-hippocampus GMV in MDD subtypes were associated with specific genes, particularly *SYTL2* for FEDN and *SORCS3/SLIT2* for R-MDD.

The observed abnormalities in GMV within specific hippocampal subregions align with previous studies [49] and provide insights into potential mechanisms related to depression episodes. The hippocampal tail is recognized as a critical region related to perception function in the pathobiology of MDD, as indicated by numerous studies [50, 51]. The hippocampal body, primarily linked to cognitive functions [36], demonstrates GMV reductions correlated with poor executive functioning in MDD. Therefore, decreased GMV in the hippocampal tail of FEDN and the hippocampal body of R-MDD may be associated with impairments of patients' sensorimotor and cognitive functions. Interestingly, the increased GMV in the hippocampal tail of R-MDD, but not FEDN, may be related to depressive severity rather than medication effects, as supported by the correlation analysis indicating larger GMV is associated with more severe depression and anxiety. However, this increase was not

(See figure on next page.)

**Fig. 1** The overview of data analysis in this study. We first integrated GMV data from the T1-weighted images and GE data from the AHBA ex-vivo dataset, identifying the genes related to hippocampal GMV. Then we validated these genes using an in-vivo dataset from healthy controls and explored GMV differences between patients and controls. Finally, we investigated gene profiles associated with GMV differences between FEDN and R-MDD by combining both prior-knowledge and data-driven MDD- and HP-related genes. MDD: major depressive disorder; GMV: gray matter volume; GE: gene expression; HP: hippocampus

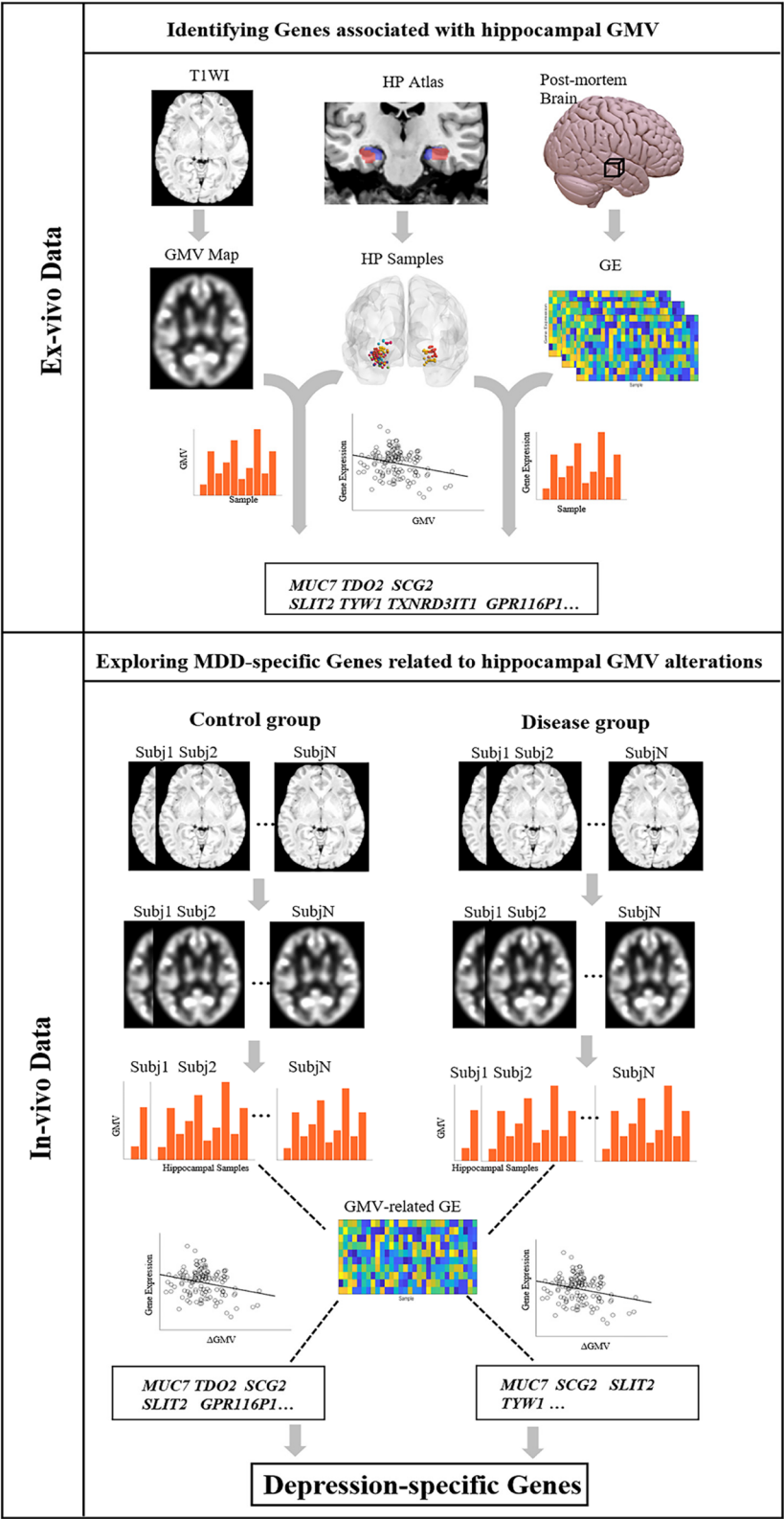


**Fig. 1** (See legend on previous page.)

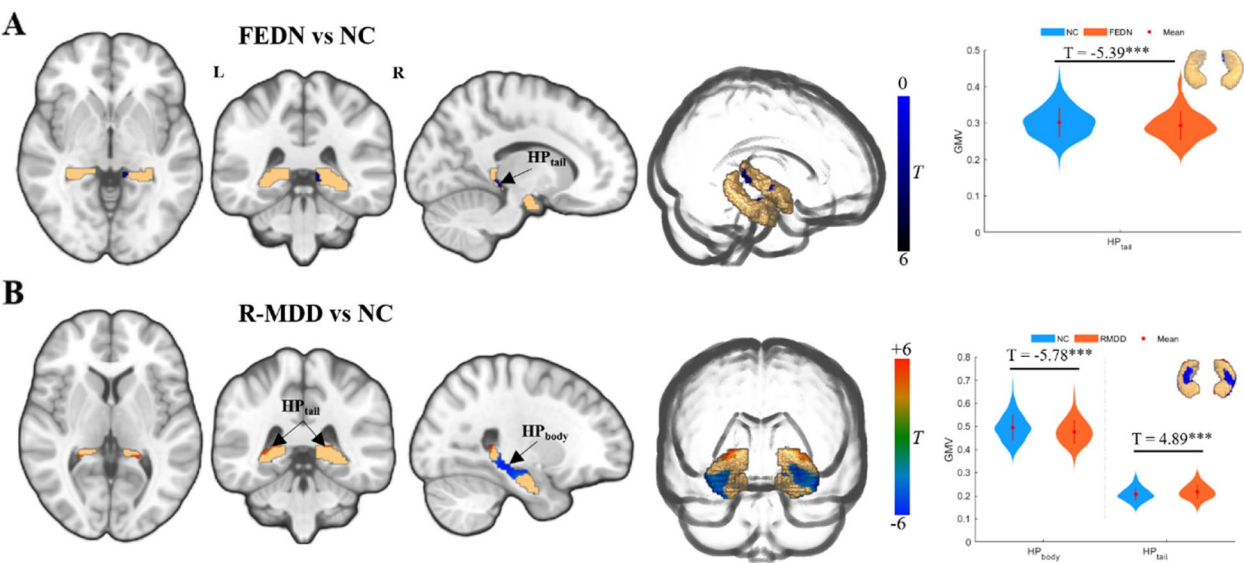


**Fig. 2** The group comparisons in hippocampal GMV. A and B show voxel-wise GMV alterations within hippocampus in FEDN and R-MDD groups compared to NC group, respectively. The positive and negative t values represent a larger and smaller GMV in disease group than NC group, respectively (\*\*\*) represents  $p < 0.001$ . FEDN: first-episode drug-naïve; R-MDD: recurrent major depressive disorder; NC: normal control; HP: hippocampus; GMV: gray matter volume

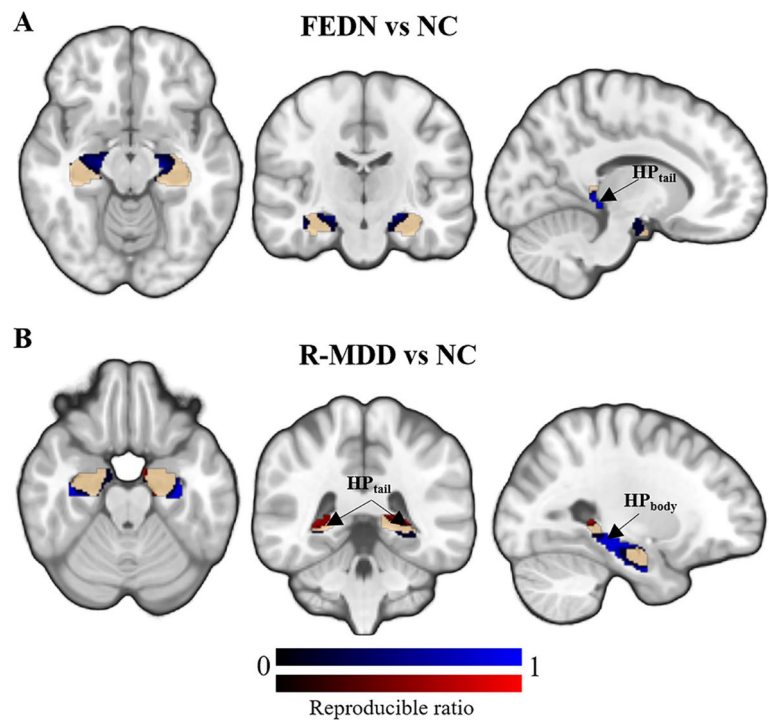


**Fig. 3** The results of reproducibility analysis for group comparisons. We performed Leave-One-Site-Out Cross Validation (LOSOCV) for each paired group comparison to assess the reproducibility of GMV differences between groups, conducting five tests for FEDN vs. NC and six tests for R-MDD vs. NC, respectively. Reproducible ratio represents the proportion of the number of tests with significant differences in the total number of tests. The red and blue colors represent increased and decreased GMV in disease group than NC group, respectively.

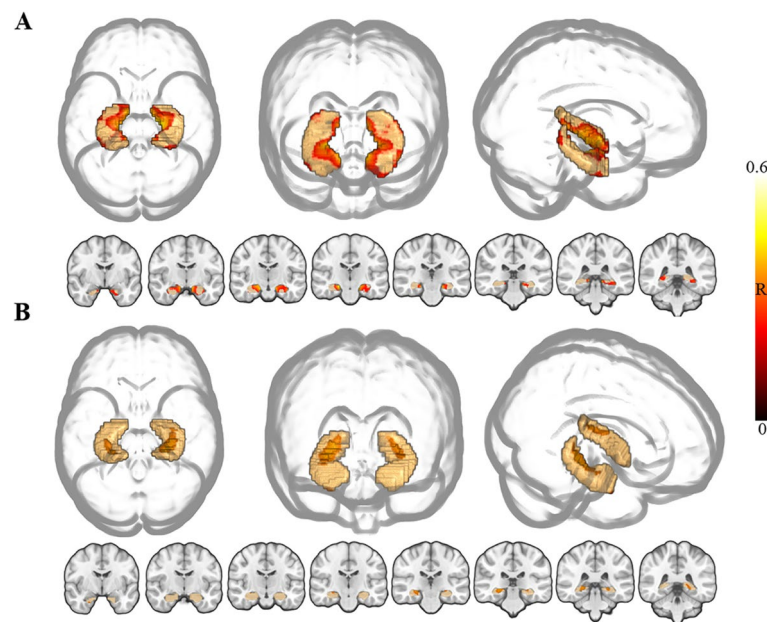


**Fig. 4** Voxel-wise correlations between the hippocampal GMV and the clinical assessments. A and B represent correlations between hippocampal GMV and score of item 8 of HAMD-17 and total score of HAMA, respectively

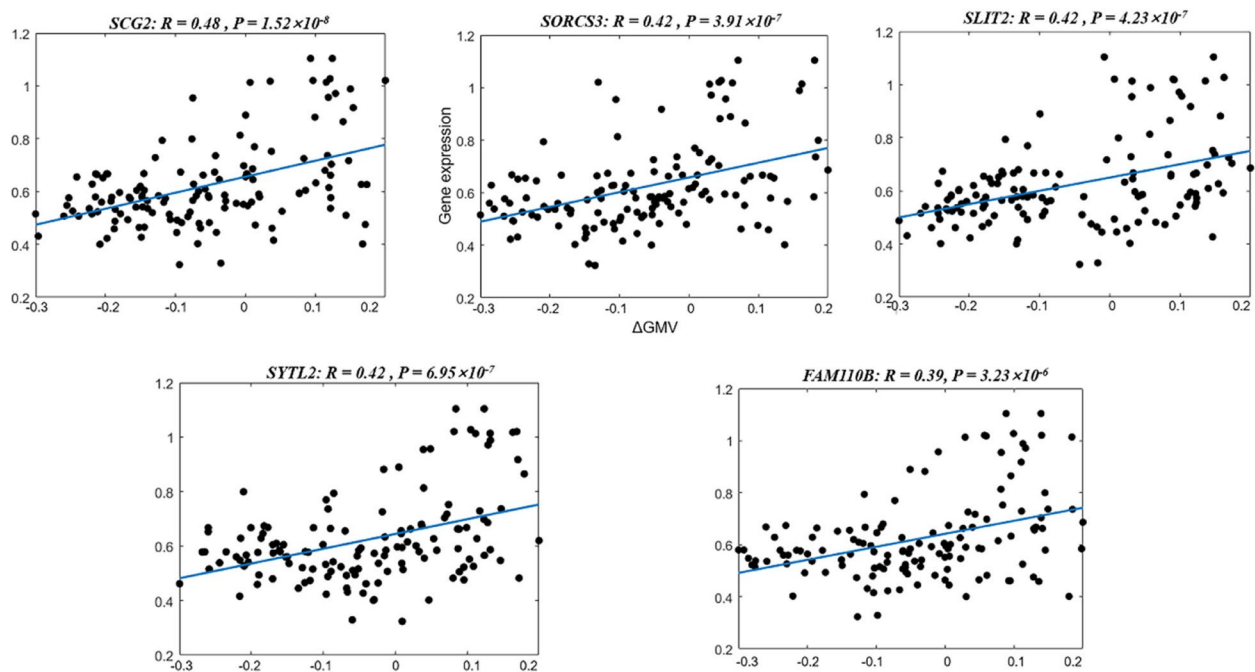


**Fig. 5** Correlations between  $\Delta$ GMV and gene expression. The  $\Delta$ GMV, for SYTL2, SORCS3/SLIT2, and SCG2/FAM110B, represents the differences between FEDN and NC, between R-MDD and NC, and between R-MDD and FEDN, respectively

found in the FEM group compared to FEDN, suggesting that depressive episodes may be a contributing factor. Prior studies reported reduced hippocampal volume in patients with multiple episodes of depression, but

not in first-episode patients, and a negative correlation between hippocampal volume and current episode duration has been noted [4, 15]. In addition, consistent with a prior study [52], the current study did not find significant



**Table 1** Genes associated with GMV differences between MDD subtypes and NC

Gene Name	Full name	Chr	Biological Function	References
<i>SORCS3</i>	sortilin related VPS10 domain containing receptor 3	10	This gene may be involved in the calcium-dependent regulation of rhodopsin phosphorylation and may be of relevance for neuronal signaling in the central nervous system.	[30, 37, 38]
<i>SCG2</i>	secretogranin II	2	This gene is involved in the packaging or sorting of peptide hormones and neuropeptides into secretory vesicles.	[39–41]
<i>SLIT2</i>	slit guidance ligand 2	4	This gene plays a highly conserved role in axon guidance and neuronal migration, and also has functions during other cell migration processes including leukocyte migration.	[39, 42, 43]
<i>SYTL2</i>	synaptotagmin like 2	11	This gene facilitates vesicle trafficking necessary for long-term potentiation, allowing neurons to communicate effectively through synapses, and its deficiency may lead to severe impairments in synaptic transmission.	[44, 45]
<i>FAM110B</i>	family with sequence similarity 110 member B	8	Functional and expression analyses suggest that the <i>FAM110</i> family might be associated with the cell cycle.	[46–48]

correlations between intra-hippocampus GMV and illness duration.

At the microstructural level, vesicle trafficking, crucial for synaptic transmission and plasticity, is implicated in depression [53]. Chronic stress is known to impair long-term potentiation (LTP) in the hippocampus, thereby affecting memory function [54]. Within this context, the synaptotagmin-like (SYTL) protein family plays a pivotal role in membrane trafficking [55]. Specifically, *SYTL2*, a member of this family, facilitates vesicle trafficking essential for LTP formation, enabling effective neuronal communication through synapses [45]. Deficiency in *SYTL2* leads to severe disruptions in synaptic transmission [56]. Furthermore, during high-frequency activity, while short-term depression may initially decrease synaptic release, recovery can result in short-term enhancement [57]. The correlation between *SYTL2* expression and GMV suggests that macroscale hippocampal atrophy in familial early-onset MDD (FEDN) could be linked to microscale synaptic damage.

The *SORCS3* gene, exclusively expressed in the nervous system and localized to the postsynaptic density, is induced by neuronal activity in the hippocampus [38, 58]. Recent GWAS analyses have associated *SORCS3* with MDD risk, identifying it as a significant gene in excitatory synaptic pathways [59, 30]. Mice deficient in *SORCS3* exhibit impaired long-term depression and altered hippocampus-dependent memory and learning [60]. Additionally, *SORCS3* is a crucial regulator of synaptic transmission and plasticity, particularly in controlling the proper positioning and mobility of glutamate receptors in the postsynaptic density. Post-mortem studies of the hippocampus in MDD patients have demonstrated disruptions in synaptic and glutamatergic signaling pathways, implicating these abnormalities in MDD pathology [61]. A study involving young adults with depression also

indicated a significant increase in hippocampal glutamate levels [62]. Collectively, these findings hint at a potential association between *SORCS3* and hippocampal GMV alterations in R-MDD, particularly in relation to synaptic and glutamate signaling abnormalities.

The *SLIT2* gene encodes a member of the slit family of secreted glycoproteins, which act as ligands for the roundabout (Robo) family of immunoglobulin receptors. *SLIT2* regulates axonal guidance, branching, and neural migration through its interactions with Robo [63]. Studies on *SLIT2*-deficient mice have shown that its absence leads to axonal defasciculation [39, 42]. As a repellent guidance molecule, *SLIT2* exerts effects on hippocampal axons, which are associated with recurrent mossy fiber sprouting in the human hippocampus. Increasing evidence suggests that *SLIT2* overexpression displays hallmarks of Alzheimer’s disease, including hippocampal neuron apoptosis and A $\beta$  protein deposition [43], and produces depression-like behaviors linked to neuronal impairment and molecular alterations in the hippocampus [64]. Thus, the correlation between *SLIT2* expression and hippocampal GMV may indicate axonal microstructural impairments underlying these volume changes in R-MDD.

Secretogranin II (*SCG2*), predominantly expressed in the central nervous system [39], is involved in sorting and packaging peptide hormones and neuropeptides into secretory vesicles [65]. It is mainly localized at mossy fiber terminals in the hippocampus and climbing fibers in the cerebellum, with expression accumulating in parvalbumin-positive interneurons [66]. This gene has been proposed as a cerebrospinal fluid (CSF) biomarker for mild cognitive impairment, bipolar disorder, and developmental delay [67]. Overexpression or knockdown of *SCG2* in hippocampal neurons significantly affects dendritic arborization and synaptic formation [41]. A

recent study has demonstrated that *SCG2* plays a role in the plasticity mechanisms of inhibitory synapses, and its reorganization of inhibitory synaptic input may influence network function in vivo [68]. Additionally, functional and expression analyses suggest that the *FAM110* family, of which *FAM110B* is a member, might be linked to the cell cycle [46], with expression observed in tissues such as the spleen and brain. *FAM110B* has been associated with schizophrenia and bipolar disorder [47, 69], although research on this gene within the brain remains limited.

Taken together, the observed GMV abnormalities in MDD subtypes may be driven by complex interactions at the synaptic and axonal levels, involving genes such as *SYTL2*, *SORCS3*, *SLIT2*, and *SCG2*. Future longitudinal studies are needed to explore how these intra-hippocampal GMV changes evolve over the course of depressive episodes, providing deeper insights into the underlying mechanisms and clinical implications of MDD.

### Limitation

Several limitations should be noted in this study. First, the gene expression and MRI data of MDD used for the transcriptomic-neuroimaging association analysis were not derived from the same individuals. While previous studies have shown that gene expression profiles exhibit relatively conserved spatial patterns across brain structures among individuals, caution is warranted when interpreting results from cross-individual association analyses. Second, the GMV-related genes were identified indirectly through transcription-neuroimaging spatial correlation analysis rather than through experimental validation. Future animal studies are recommended to confirm our preliminary findings. Third, the unavailability of medication history for the R-MDD group raises the possibility that their HAMD assessment scores could be influenced by prior drug treatment. It is imperative that this factor be taken into account and controlled for in future studies on MDD. Finally, GMV does not encompass all aspects of intra-hippocampal structure. Genetic mechanisms underlying other measures of hippocampal morphology, such as thickness and surface area [70, 71], are also important and warrant further investigation.

### Conclusion

This study utilized a combined transcriptomic-neuroimaging approach to explore abnormal changes in intra-hippocampus GMV in MDD subtypes, and their associations with specific genes. Results revealed distinct GMV patterns between different subtypes, with FEDN showing decreased GMV in the left hippocampal tail and R-MDD exhibiting decreased GMV in the bilateral hippocampal body but increased GMV in the bilateral hippocampal

tail. Furthermore, GMV alterations in FEDN were potentially associated with the *SYTL2* gene, while those in R-MDD were related to the *SORCS3/SLIT2* genes. These findings not only highlight the unique neurobiological signatures of FEDN and R-MDD but also suggest potential clinical implications for targeted gene-based therapies in MDD subtypes.

### Supplementary Information

The online version contains supplementary material available at <https://doi.org/10.1186/s12888-025-06562-4>.

Additional file 1.

### Acknowledgements

None.

### Authors' contributions

F.F. Sun and Z.Y. Zhao wrote the main manuscript text. Y.F. Shuai, J.R. Wang and J. Yan prepared Figs. 1, 2, 3 and 4. B. Lin and X.Y. Li prepared Fig. 5; Table 1. F.F. Sun and Z.Y. Zhao conceptualized this work and review & editing the manuscript. All authors reviewed the manuscript.

### Funding

This work was supported by the Zhejiang Provincial Philosophy and Social Sciences Planning Project (24NDQN039YB) and Shaoxing Basic Public Welfare Program (2023A14017).

### Data availability

The data used in this study, including the imaging and collateral data, were obtained from the REST-meta-MDD Project. This project is publicly available and open-access. To access these data, interested parties can register at <http://rfmri.org/REST-meta-MDD>.

### Declarations

#### Ethics approval and consent to participate

All study sites obtained approval from their local institutional review boards and ethics committees, including the Ethics Committee of the Sir Run Run Shaw Hospital, School of Medicine, Zhejiang University, and the Affiliated Hospital of Hangzhou Normal University; the Institutional Review Board of China Medical University; the ethics committee of The First Affiliated Hospital of Jinan University; the ethics committee of the First Affiliated Hospital of Chongqing Medical University; the Institutional Review Board of the Central South University; the local ethics committees of the Anhui Medical University; the Research Ethics Committee of the Brain Imaging Center of Southwest University and First Affiliated Hospital of Chongqing Medical School; the Institutional Review Board of Taipei Veterans General Hospital; the Institutional Review Board of China Medical University, the Imaging Center for Brain Research, Beijing Normal University; the Institutional Review Board of Anding Hospital, Capital Medical University, and the Ethics Committee of Sichuan University, and followed the principles of the Declaration of Helsinki, and all participants provided written informed consent.

#### Consent for publication

Not applicable.

#### Competing interests

The authors declare no competing interests.

#### Author details

<sup>1</sup>Center for Brain, Mind and Education, Shaoxing University, Shaoxing, China. <sup>2</sup>Department of Psychology, Shaoxing University, Shaoxing, China. <sup>3</sup>Key Laboratory for Biomedical Engineering of Ministry of Education, Department of Biomedical Engineering, College of Biomedical Engineering & Instrument Science, Zhejiang University, Hangzhou, China. <sup>4</sup>Department of Radiology, The

Second Affiliated Hospital, Zhejiang University School of Medicine, Hangzhou, China. <sup>5</sup>School of Rehabilitation, Hangzhou Medical College, Hangzhou, China. <sup>6</sup>Children's Hospital, Zhejiang University School of Medicine, National Clinical Research Center for Child Health, Binjiang Campus, 3333 Binsheng Rd, Hangzhou, China.

Received: 21 November 2024 Accepted: 31 January 2025

Published online: 15 February 2025

## References

- Rosene DL, Van Hoesen GW. The hippocampal formation of the primate brain: a review of some comparative aspects of cytoarchitecture and connections. *Cerebral cortex: further aspects of cortical function, including hippocampus*. 1987. p. 345–456.
- Salloway S, Cummings J. Subcortical disease and neuropsychiatric illness [J]. *J Neuropsychiatry Clin Neurosci*. 1994;6(2):93–9.
- Soares JC, Mann JJ. The anatomy of mood disorders—review of structural neuroimaging studies [J]. *Biol Psychiatry*. 1997;41(1):86–106.
- Maller JJ, Broadhouse K, Rush A J, Gordone, Grieve Koslows. Increased hippocampal tail volume predicts depression status and remission to anti-depressant medications in major depression [J]. *Mol Psychiatry*. 2018;23(8):1737–44.
- Campbell S, Marriott M, Nahmias C, Macqueen GM. Lower hippocampal volume in patients suffering from Depression: a Meta-analysis [J]. *Am J Psychiatry*. 2004;161(4):598–607.
- Videbech P. Hippocampal volume and depression: a Meta-analysis of MRI studies [J]. *Am J Psychiatry*. 2004;161(11):1957–66.
- Kronmüller K-T, Schröder J, Köhler S, Götz B, Victor D, Giesel Ungerj, Magnotta F, Mundt V, Essig C. Hippocampal volume in first episode and recurrent depression [J]. *Psychiatry Research: Neuroimaging*. 2009;174(1):62–6.
- Macqueen G M Campbells, McEwen B S, Macdonald K, Amano S, Joffe R T, Nahmias C. Young L T. Course of illness, hippocampal function, and hippocampal volume in major depression [J]. *Proceed Nat Acad Sci*. 2003; 100(3):1387–92.
- Neumeister A, Wood S, Bonne O, Nugent A C, Luckenbaugh D A, Young T, Bain E E, Charney D S. Drevets W C. reduced hippocampal volume in unmedicated, remitted patients with major depression versus control subjects [J]. *Biol Psychiatry*. 2005;57(8):935–7.
- Veltman D J Schmaall, Van Erp T G M, Sämann PG, Frodl T, Jahanshad N, Tiemeier Loehrere. Hofman A, Niessen W J. Subcortical brain alterations in major depressive disorder: findings from the ENIGMA Major Depressive disorder working group [J]. *Mol Psychiatry*. 2016;21(6):806–12.
- Robinson JL, Barron D S, Kirby L A J, Bottenhorn K L, Hill A C, Murphy J E, Katz J S. Salibi N, Eickhoff S B, Fox P T. Neurofunctional topography of the human hippocampus [J]. *Hum Brain Mapp*. 2015;36(12):5018–37.
- Zarei M, Beckmann C F, Binnewijzend M A A, Schoonheim M M, Oghabian M A, Sanz-arigita E J, Scheltens P, Matthews P M, Barkhof F. Functional segmentation of the hippocampus in the healthy human brain and in Alzheimer's disease [J]. *NeuroImage*. 2013;66:28–35.
- Vos de Wael R, Larivière S, Hong S-J, Caldairoub, Margulies D S, Jefferies E, Bernasconi A, Smallwood J. Bernasconi N, Bernhardt B C. Anatomical and microstructural determinants of hippocampal subfield functional connectome embedding [J]. *Proceed Nat Acad Sci*. 2018; 115(40):10154–9.
- Roddy D W, Farrell C, Doolin K, Roman E, Tozzi L, Frodl T, O'Keane V, O'Hanlon E. The Hippocampus in Depression: more than the Sum of its parts? Advanced hippocampal substructure segmentation in Depression [J]. *Biol Psychiatry*. 2019;85(6):487–97.
- Macqueen GM, Yucel K, Taylor V H, Macdonald K. Posterior hippocampal volumes are Associated with Remission Rates in patients with major depressive disorder [J]. *Biol Psychiatry*. 2008;64(10):880–3.
- Gonul AS, Kitis O, Eker M C, Eker O D Ozane. Association of the brain-derived neurotrophic factor Val66Met polymorphism with hippocampus volumes in drug-free depressed patients [J]. *World J Biol Psychiatry*. 2011;12(2):110–8.
- Eker MC, Kitis O, Eker O D, Ozan Okurh. Akarsu N, Gonul A S. smaller Hippocampus volume is Associated with short variant of 5-HTTLPR polymorphism in medication-free major depressive disorder patients [J]. *Neuropsychobiology*. 2010;63(1):22–8.
- Han K-M Wone, Kang J, Choi S, Kim A, Lee M-S, Tae W-S. Ham B-J. TESC gene-regulating genetic variant (rs7294919) affects hippocampal subfield volumes and parahippocampal cingulum white matter integrity in major depressive disorder [J]. *J Psychiatry Res*. 2017;93:20–9.
- Mikolas P, Tozzi L, Doolin K, Farrell C, O'Keane V Frodl. Effects of early life adversity and FKBP5 genotype on hippocampal subfields volume in major depression [J]. *J Affect Disord*. 2019;252:152–9.
- Stratmann M, Konrad C, Kugel H, Krug A, Schöning S, Ohrmann P, Uhlmann C, Postert C, Suslow T. Insular and hippocampal Gray Matter volume reductions in patients with major depressive disorder [J]. *PLoS ONE*. 2014;9(7):e102692.
- Hawrylycz M, Miller J A, Menon V, Feng D, Dolbeare T, Guillozet-Bongaarts A L, Jegga A G, Aronow B J. Canonical genetic signatures of the adult human brain [J]. *Nat Neurosci*. 2015;18(12):1832–44.
- Xie Y, Zhang X, Liu F, Qin W, Fu J, Xue K. Brain mRNA expression Associated with cortical volume alterations in Autism Spectrum disorder [J]. *Cell Rep*. 2020;32(11):108137.
- Romme I A C, DE Reus M A, Ophoff R A, Kahn R S, Van den Heuvel. M P. Connectome Disconnectivity and cortical gene expression in patients with Schizophrenia [J]. *Biol Psychiatry*. 2017;81(6):495–502.
- Fu J, Liu F, Qin W, Xu Q, Yu C, INITIATIVE A S D. N. Individual-Level Identification of Gene expression Associated with volume differences among neocortical areas [J]. *Cereb Cortex*. 2020;30(6):3655–66.
- Martins D, Giacomel A, Williams S C R, Turkheimer F, Dipasquale O Veronesem. Imaging transcriptomics: convergent cellular, transcriptomic, and molecular neuroimaging signatures in the healthy adult human brain [J]. *Cell Rep*. 2021;37(13):110173.
- Yan C-G, Chen X, Castellanos F X Lil, Bai T-J, BO Q-J Caoj. Chen G-M. Reduced default mode network functional connectivity in patients with recurrent major depressive disorder [J]. *Proceed Nat Acad Sci*. 2019; 116(18):9078–83.
- Xue K, Guo L, Zhu W, Liang S, Xu Q, Ma L, Liu M, Zhang Y, Liu F. Transcriptional signatures of the cortical morphometric similarity network gradient in first-episode, treatment-naïve major depressive disorder [J]. *Neuropsychopharmacology*. 2023;48(3):518–28.
- Mao H, Xu M, Wang H, Liu Y, Wang F, Gao Q, Zhao S, Hu Mal, Zhang X. Transcriptional patterns of brain structural abnormalities in CSVD-related cognitive impairment [J]. *Front Aging Neurosci*. 2024;16:1503806.
- Fan L, Li H, Zhuo J, Zhang Y, Wang J, Chen L, Yang Z, Chu C, Xie S, Laird A R. The human Brainnetome Atlas: a New Brain Atlas based on Connective Architecture [J]. *Cereb Cortex*. 2016;26(8):3508–26.
- Wray N R, Ripke S, Mattheisen M, Trzaskowski M, Byrne E M, Abdellaoui A, Adams M J, Agerbo E. Air T M. Genome-wide association analyses identify 44 risk variants and refine the genetic architecture of major depression [J]. *Nat Genet*. 2018;50(5):668–81.
- Hibar D P, Adams H H H, Jahanshad N, Chauhan G, Stein J L, Hofer E, Renteria M E, Bis J C, Arias-Vasquez A, Ikram M. Novel genetic loci associated with hippocampal volume [J]. *Nat Commun*. 2017;8:13624.
- Van der Meer D, Rokicki J, Kaufmann T, Córdova-Palomera A, Moberget T, Alnæs D, Bettella F, Frei O, Doan N T, Sønderby IE, et al. Brain scans from 21,297 individuals reveal the genetic architecture of hippocampal subfield volumes [J]. *Mol Psychiatry*. 2020;25(11):3053–65.
- Meng X, Navoly G, Giannakopoulou O, Levey D F, Koller D, Pathak G A, Koen N, Lin K, Adams M J, Renteria ME, et al. Multi-ancestry genome-wide association study of major depression aids locus discovery, fine mapping, gene prioritization and causal inference [J]. *Nat Genet*. 2024;56(2):222–33.
- Burt JB, Helmer M, Shinn M. Murray J D. Generative modeling of brain maps with spatial autocorrelation [J]. *NeuroImage*. 2020;220:117038.
- Zhao Z, Cai H, Zheng W, Liu T, Sun D, Han G, Zhang Y. Atrophic pattern of hippocampal subfields in Post-stroke demented patient [J]. *J Alzheimers Dis*. 2021;80(3):1299–309.
- Zhao Z, Cai H, Huang M, Zheng W, Liu T, Sun D, Han G, Ni L, Zhang Y. Altered functional connectivity of hippocampal subfields in Poststroke dementia [J]. *J Magn Reson Imaging*. 2021;54(4):1337–48.
- Kamran M, Laighneach A, Bibi F, Donohoe G, Ahmed N, Rehman A U. Morris D W. Independent Associated SNPs at SORCS3 and its protein interactors for multiple brain-related disorders and traits [J]. *Genes*. 2023;14(2):482.
- Christiansen G B, Andersen K H, Riis S, Nykjaer A, Bolcho U, Jensen M S, Holm M M. The sorting receptor SorCS3 is a stronger regulator of

- glutamate receptor functions compared to GABAergic mechanisms in the hippocampus [J]. *Hippocampus*. 2017;27(3):235–48.
39. Plump AS, Erskine L, Sabatier C, Brose K, Epstein C J, Goodman C S, Mason C A. Tessier-Lavigne M. Slit1 and Slit2 cooperate to prevent premature midline crossing of retinal axons in the mouse visual system [J]. *Neuron*. 2002;33(2):219–32.
  40. Courel M, Vasquez M S, Hook V Y, Mahata S K, Taupenot L. Sorting of the Neuroendocrine Secretory Protein Secretogranin II into the Regulated Secretory Pathway: ROLE OF N- AND C-TERMINAL  $\alpha$ -HELICAL DOMAINS \* [J]. *J Biol Chem*. 2008;283(17): 11807–22.
  41. Lim S-H, Sung Y-J, JO N, Lee N-Y, Kim K-S, Lee D Y, Kim N-S Leej, Byun J-Y, Shin, Y-B, et al. Nanoplasmonic immunosensor for the detection of SCG2, a candidate serum biomarker for the early diagnosis of neurodevelopmental disorder [J]. *Sci Rep*. 2021;11(1):22764.
  42. Shu T, Sundaresan V, McCarthy M M, Richards L J. Slit2 guides both precrossing and postcrossing callosal axons at the midline in vivo [J]. *J Neurosci*. 2003;23:8176–84.
  43. Li JC, Wen Y X Hanl, Yang Y X, Li S, Li X S, Zhao C J, Wang T Y, Chen H, Liu Y, et al. Increased permeability of the blood-brain barrier and Alzheimer's disease-like alterations in slit-2 transgenic mice [J]. *J Alzheimers Dis*. 2015;43(2):535–48.
  44. Pang Z P, Melicoff E, Padgett D, Liu Y, Teich A F, Dickey B F, Lin W, Adachi R, Südhof T C. Synaptotagmin-2 Is Essential for Survival and Contributes to  $\text{Ca}^{2+}$ -Triggering of Neurotransmitter Release in Central and Neuromuscular Synapses [J]. *J Neurosci*. 2006; 26(52): 13493.
  45. Aktar S, Ferdousi F, Kondo S, Kagawa T. Transcriptomics and biochemical evidence of trigonelline ameliorating learning and memory decline in the senescence-accelerated mouse prone 8 (SAMP8) model by suppressing proinflammatory cytokines and elevating neurotransmitter release [J]. *Geroscience*. 2024;46(2):1671–91.
  46. Hauge H, Patzke S. Aasheim H-C. characterization of the FAM110 gene family [J]. *Genomics*. 2007;90(1):14–27.
  47. Wang K-S, Liu X-F Aragamn. A genome-wide meta-analysis identifies novel loci associated with schizophrenia and bipolar disorder [J]. *Schizophr Res*. 2010;124(1):192–9.
  48. Consortium WTC-C Peic. A Genome-Wide Association Analysis of a broad psychosis phenotype identifies three loci for further investigation [J]. *Biol Psychiatry*. 2014;75(5):386–97.
  49. Schenck JF. The role of magnetic susceptibility in magnetic resonance imaging: MRI magnetic compatibility of the first and second kinds [J]. *Med Phys*. 1996;23(6):815–50.
  50. Maller JJ, Daskalakis Z J, Fitzgerald PB. Hippocampal volumetrics in depression: the importance of the posterior tail [J]. *Hippocampus*. 2007;17(11):1023–7.
  51. Malykhin N V, Lebel R M, Coupland N J, Wilman A H, Carter R. In vivo quantification of hippocampal subfields using 4.7 T fast spin echo imaging [J]. *NeuroImage*. 2010;49(2):1224–30.
  52. Macqueen G M Campbells, MCewen B S, Macdonald K, Amano S, Joffe R T, Nahmias C. Young L T. course of illness, hippocampal function, and hippocampal volume in major depression [J]. *Proc Natl Acad Sci U S A*. 2003;100(3):1387–92.
  53. Zhang, C-C, Zhu L-X, Shi H-J, Zhu L-J. The role of vesicle release and synaptic transmission in Depression [J]. *Neuroscience*. 2022;505:171–85.
  54. Balu D T, Lucki I. Adult hippocampal neurogenesis: regulation, functional implications, and contribution to disease pathology [J]. *Neurosci Biobehav Rev*. 2009;33(3):232–52.
  55. Elferink L A, Peterson M R, Scheller R. H. A role for synaptotagmin (p65) in regulated exocytosis [J]. *Cell*. 1993;72(1):153–9.
  56. Pang Z P, Melicoff E, Padgett D, Liu Y, Teich A F, Dickey B F, Lin W, Adachi R, Südhof T C. Synaptotagmin-2 is essential for survival and contributes to  $\text{Ca}^{2+}$  triggering of neurotransmitter release in central and neuromuscular synapses [J]. *J Neurosci*. 2006;26(52):13493–504.
  57. Genc O, Kochubey O, Toonen R F, Verhage M. Munc18-1 is a dynamically regulated PKC target during short-term enhancement of transmitter release [J]. *Elife*. 2014;3:e01715.
  58. Hermey G, Mahlke C, Gutzmann J J, Schreiber J, BLüthgen N. Genome-wide profiling of the activity-dependent hippocampal transcriptome [J]. *PLoS ONE*. 2013;8(10):e76903.
  59. Howard D M, Adams M J, Shiralil M, Clarke T K, Marioni R E, Davies G, Coleman J R I, Alloza C, Shen X, Barbu M C. Genome-wide association study of depression phenotypes in UK Biobank identifies variants in excitatory synaptic pathways [J]. *Nat Commun*. 2018;9(1):1470.
  60. Breiderhoff T, Christiansen G B, Pallesen L T, Vaegter C, Nykjaer A, Holm M M, Glerup S, Willnow T E. Sortilin-related receptor SORCS3 is a postsynaptic modulator of synaptic depression and fear extinction [J]. *PLoS ONE*. 2013;8(9):e75006.
  61. Duric V, Banasr M, Stockmeier C A, Simen A A, Newton S S, Overholser J C, Jurjus G J Dieterl. Duman R S. altered expression of synapse and glutamate related genes in post-mortem hippocampus of depressed subjects [J]. *Int J Neuropsychopharmacol*. 2013;16(1):69–82.
  62. Hermens D F, Chitty K M, Lee R S, Tickell A, Haber P S, Naismith S L, Hickie I B Lagopoulos. Hippocampal glutamate is increased and associated with risky drinking in young adults with major depression [J]. *J Affect Disord*. 2015;186:95–8.
  63. Fang M, Liu G W, Pan Y M Shenl, Li C S, Xi Z Q, Xiao F, Wang L, Chen D. Wang X F. abnormal expression and spatiotemporal change of Slit2 in neurons and astrocytes in temporal lobe epileptic foci: a study of epileptic patients and experimental animals [J]. *Brain Res*. 2010;1324:14–23.
  64. Huang G, Wang S, Li Yanj, Feng C, Chen J, Zheng Q, Li X, He H, Young Y. Depression-/Anxiety-Like Behavior alterations in adult Slit2 transgenic mice [J]. *Front Behav Neurosci*. 2020;14:622257.
  65. Courel M, Vasquez M S, Hook V Y, Mahata S K Taupenotl. Sorting of the neuroendocrine secretory protein secretogranin II into the regulated secretory pathway: role of N- and C-terminal  $\alpha$ -helical domains [J]. *J Biol Chem*. 2008;283(17):11807–22.
  66. Miyazaki T, Yamasaki M, Uchigashima M, Matsushima A, Watanabe M. Cellular expression and subcellular localization of secretogranin II in the mouse hippocampus and cerebellum [J]. *Eur J Neurosci*. 2011;33(1):82–94.
  67. Jakobsson J, Stridsberg M, Zetterberg H, Blennow K, Ekman C J, Johansson A G, Sellgren C, Landén M. Decreased cerebrospinal fluid secretogranin II concentrations in severe forms of bipolar disorder [J]. *J Psychiatry Neurosci*. 2013;38(4):E21–6.
  68. Yap E L, Pettit N L, Davis C P, Nagy M A, Harmin D A, Golden E, Dagliyan O, Lin C, Rudolph S, Sharma N, et al. Bidirectional perisomatic inhibitory plasticity of a Fos neuronal network [J]. *Nature*. 2021;590(7844):115–21.
  69. Bramon E, Pirinen M, Strange A, Lin K, Freeman C, Bellenguez C, Su Z, Band G, Pearson R. A genome-wide association analysis of a broad psychosis phenotype identifies three loci for further investigation [J]. *Biol Psychiatry*. 2014;75(5):386–97.
  70. Dekraker J, Köhler S. Khan A R. Surface-based hippocampal subfield segmentation [J]. *Trends Neurosci*. 2021;44(11):856–63.
  71. DeKraaker J, Haast RAM, Yousif MD, et al. Automated hippocampal unfolding for morphometry and subfield segmentation with HippUnfold. *Elife*. 2022;11:e77945.

## Publisher's Note

Springer Nature remains neutral with regard to jurisdictional claims in published maps and institutional affiliations.